# POLYMER NANOFIBER-BASED ELECTRIC ACTUATORS REINFORCED BY MONODISPERSE BARIUM TITANATE COLLOIDAL NANOCRYSTALS

Soheil Malekpour

A thesis submitted in partial fulfillment of
requirements for the degree of
Master of Science

Department of Chemistry and Biochemistry

Central Michigan University
Mount Pleasant, Michigan
May 2016

ACKNOWLEDGEMENTS

I would like to thank all the people who helped me with this research project, in particular Dr. Axel Mellinger and Dr. Saman Salemizadeh Parizi, my family for their supports and encouragements through my master degree. I am also very grateful to my committee members Dr. Bob Howell and Dr. Brad Fahlman who made me successful in writing this thesis.

Last but not least, I would like to express my special gratitude to my advisor Dr. Gabriel Caruntu who guided and supported me throughout this thesis. I am really happy that I had the chance to write this thesis under his supervision and I always will be grateful of his advice.

ABSTRACT

POLYMER NANOFIBER-BASED ELECTRIC ACTUATORS REINFORCED BY MONODISPERSE BARIUM TITANATE COLLOIDAL NANOCRYSTALS

by Soheil Malekpour

Electric actuators are devices which can convert electrical energy into a mechanical torque. These functional devices incorporate smart materials that can be potentially used as artificial muscles in technological applications whereby a muscle-like behavior is needed. Such applications include, but are not restricted to robotics, medical devices, toys and microfluidic pumps, respectively. Since natural muscles possess a fibrous structure, fiber-like structures made of a polymer and an electrostrictive material in the form of colloidal nanocrystals are very promising in terms of their physical properties, which rival those of the natural muscles and can be implemented in a wide range of technological applications.

In this research project, polymer-ceramic fiber-like structures have been fabricated by the electrospinning method and the as-spun fiber mats have been characterized structurally, compositionally and morphologically and their mechanical properties have been investigated for potential use as artificial muscles. To this end, poly(vinylidene fluoride-co-hexafluoropropylene), an electroactive polymer, and barium titanate ($BaTiO_3$), an archetypal ferroelectric an piezoelectric material, have been selected to fabricate hybrid organic inorganic system with a fiber-like morphology which provides the best combination of properties for true muscle-like behavior. The effect of addition of $BaTiO_3$ colloidal nanocrystals on the structure and properties of fibers was investigated by different experimental techniques and the performance of the polymer nanofibers reinforced by $BaTiO_3$ colloidal nanocrystals for potential use as artificial muscles were studied.

TABLE OF CONTENTS

LIST OF TABLES

TABLE PAGE

LIST OF FIGURES

FIGURE PAGE

# CHAPTER I

## ARTIFICIAL MUSCLES

Artificial muscles are one of the recent topics which have garnered the interest of many researchers in physics, chemistry, nanotechnology, materials science and biology. These devices are conventionally classified as electric actuators. Different types of actuators have been developed so far, these include: thermal, hydraulic, pneumatic, magnetic and electric based actuators. Since the topic of this research is related to the electrical properties of polymers reinforced by ceramic colloidal nanocrystals, the electric actuators are being studied in more detail.

By definition, an actuator is a device which converts a specific type of energy into mechanical torque. In the case of an electric actuator, the electrical energy is converted to mechanical energy. This phenomenon can be used for the design of devices for muscle-like behavior applications. Artificial muscle is a generic term used for materials and/or devices which can reversibly contract, expand or rotate when subjected to the action of an external stimulus such as pressure, electric field, temperature, current and etc. Muscles in human body can be simulated by materials which present actuation properties. Muscles are special materials which can undergo a high reversible deformation. The purpose of producing artificial muscles is to mimic natural muscles behavior with the same deformation and even higher stresses and strains. Based on various studies, electric field stimulated electric actuators have the most similarity to natural muscles [1].

Artificial muscles are required to show proper mechanical and actuation properties. Flexibility, strength and dielectric properties are key parameters which should be taken into account for the design of such devices, in which flexibility and strength are responsible for the

mechanical properties and their high dielectric properties will result into a higher actuation in the presence of an electric field.

Hence, choosing the proper material for the best performance has been a challenge. Polymers as materials with both high flexibility and proper strength are the best candidates for the fabrication of artificial muscles with high performance characteristics. Among these materials, electroactive polymers have been used widely for this purpose.

Electroactive polymers are polymers which exhibit a high deformation and tolerate a large force. As a result, they can be actuated by an electric field mainly due to their special structure. Electroactive polymers are divided into two groups:

- Polymers which present a high deformation but a low strength. Typical examples of such electroactive polymers are dielectric elastomers.
- Polymers which show a low deformation but sustain high strengths. Typical examples of such electroactive polymers include electrostrictive polymers such as ferroelectric polymers or conducting polymers.

From a mechanistic point of view, the actuation in polymer artificial muscles follows two paths. The first mechanism which is observed in dielectric elastomers or actuators with a high strain rate (even >40%) consists of a simple field driven actuation resulted of electrostatic interaction between the electrodes. A low elastic modulus and high electric breakdown are two main characteristics of dielectric elastomers which can create very high strains, up to 380% at high electric fields [2]. The second mechanism consists of pulling or pushing the electric dipoles inside the polymers and has been observed in electrostrictive polymers [2]. Since the purpose of this research is the fabrication of high strength artificial muscle with a low deformation, the behavior of the second family of electroactive polymers will be studied in more detail. For

studying the properties of this group, electrostrictive polymers, one should know and understand the topic electrostriction.

## 1.1 Electrostriction

Electrostriction is an intrinsic property of all dielectric materials, associated with a slight displacement of ions in the crystal lattice upon being exposed to an external field. The orientation of charged species takes place in the way that positive ions will be displaced by the direction of the electric field, while negative ions will be displaced in the opposite direction (Figure 1).

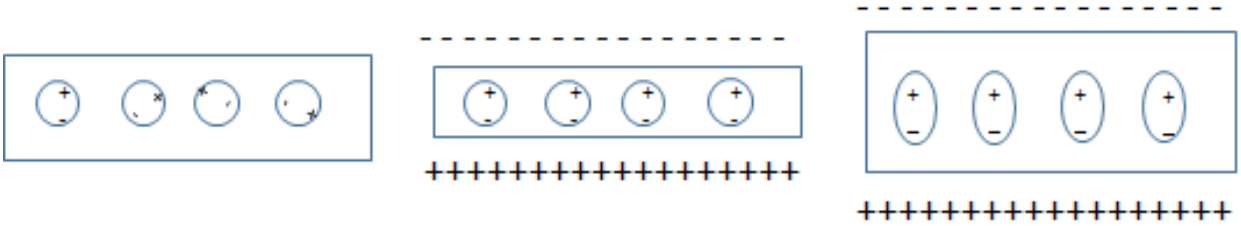

Figure 1. Illustrating the alignment of dipoles inside the sample

All insulating materials consisting more than one type of atom can be actuated in the electric field because of the difference in electronegativity of the atoms. The degree of this actuation is dependent on mechanical properties, the structure of the material, the order of difference in electronegativity and degree of polarization in the electric field. Ferroelectric polymers such as poly(vinylidene fluoride), PVDF, and its copolymers introduce strains up to 10% upon applying electric field, while for inorganic ferroelectrics such as BaTiO3 ($BaTiO_3$) strain value is in order of 0.1% [3].

As shown in Figure 2, the displacement of ions accumulates throughout the bulk material leading to an overall strain (elongation) in the direction of the applied field. The thickness will be

reduced in the orthogonal directions characterized by various physical parameters such as Poisson's ratio [4].

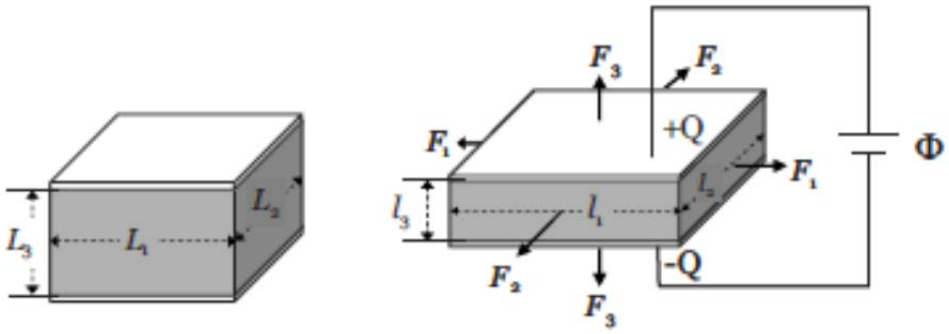


Figure 2. Actuation in the direction of electric field which will result in reduction in thickness of actuator [4]

1.2 Principle of Operation

For a better understanding of the electrostrictive behavior, a model has been designed by considering the electrostriction due to the electrostatic force imparted by the electrodes [5]. In this model the polymer is assumed as incompressible, so when the polymer film is compressed in thickness, it will expand in area and it can be said that:

$$Az = constant \quad Eq.\ (1)$$

Where $A$ and $z$ are area and thickness of the sample, respectively. Effective pressure $p$ of the actuator was defined as a change in electrostatic energy per unit area and the displacement of the film in the thickness direction:

$$p = (1/A)dU/dz \quad Eq.\ (2)$$

Where $U$ is the electrostatic energy of the film. The stored electrostatic energy $U$ of the film with opposite charges $+Q$ and $-Q$ placed on its surface can be written as:

$$U = 0.5Q^2/C = 0.5Q^2z/\varepsilon_0\varepsilon A \quad Eq.\ (3)$$

Where $C = \varepsilon_0\varepsilon A/z$ is the capacitance, $\varepsilon_0$ is the free-space permittivity ($\varepsilon_0 = 8.85\times10^{-12}Fm^{-1}$) and $\varepsilon$ is the dielectric constant of the polymer sample. The change in the stored electrostatic energy $dU$ for a change in the thickness $dz$ and a change in the area $dA$ can be derived from Equation 1 and Equation 2:

$$dU = (0.5Q^2/\varepsilon_0\varepsilon A)dz - (0.5Q^2z/\varepsilon_0\varepsilon A)dA/A \quad Eq.\ (4)$$

Applying constraints in Equation 1 will result in $dA/A = -dz/z$ and by replacing the stored energy with previously found effective pressure in actuators:

$$p = 1/AdU/dz = Q^2/\varepsilon_0\varepsilon A^2 \quad Eq.\ (5)$$

Finally, since the electric field $E$ is given by $E = Q/\varepsilon_0\varepsilon A$, an equation was derived for the effective pressure in the polymer actuators [5]:

$$p = \varepsilon_0\varepsilon E^2 \quad Eq.\ (6)$$

The actuator performance depends on both the effective pressure and strain, in which the effective pressure can be obtained by Equation 6, but the strain depends on many factors such as the Young's modulus, loading, boundary conditions etc. [5]. The simplest model for evaluating the performance of actuators is an unloaded, unconstrained case [6], in which the strain in actuators can be calculated as following:

$$S_z = -p/Y = -\varepsilon_0\varepsilon E^2/Y = -\varepsilon_0\varepsilon(V^2/z^2)/Y \quad Eq.\ (7)$$

where $S_z$ is the thickness strain, $V$ is the applied voltage and $Y$ is the Young's modulus of the sample [6]. Although the Equation 6 shows how the thickness strain in actuators can be calculated under ideal conditions, the experimental results may not exactly match the equation in some cases, it can be concluded that actuator's performance is proportional to dielectric constant and the square of the electric field.

Equations 6 and 7 provide suitable information about the choice of the materials. So far dielectric elastomers have been the most popular types of electroactive polymers for this purpose and have been used in many artificial muscles applications [7-16] due to their low elastic modulus resulting to high strain rates, (up to 380%) [17] at high electric fields. Different studies have been carried out to explore the possible applications of elastomers as electric actuators. Pei *et al.* studied the use of dielectric elastomers in biomimetic walking robots [8]. To this end, they developed electroelastomer rolls based on dielectric elastomers between compliant electrodes. These rolls could bear up to 50 times their own weight and showed 26% strain. In another study, Kovacz *et al.* analyzed the electrode properties on the surface of the dielectric elastomers and the performance of stack actuators. They saw novel and interesting properties in terms of contraction compared to those of planar actuators [9]. Carpi *et al.* studied the cylindrical electric actuators made of silicone elastomers and reported strains higher than 140% [10]. Few studies have been carried out on commercial elastomers to define their properties for this field. Plerine *et al.* used pre-straining techniques to increase the actuation in these materials. They reported strains, pressure and response time of silicone and acrylic elastomers exceeded those of natural muscles [13].

Although dielectric elastomers showed promising properties in terms of actuation, their low strength makes a challenge for utilizing these materials in applications which need higher strengths. Another drawback of this class is their low performance at low electric fields. Hence conductive and ferroelectric polymers can be proper candidates for designing artificial muscles working at low electric fields and be able to stand higher strength. Carbon nanotubes has garnered an increasing attention as a material with interesting electrical properties for use in both actuators and fillers for improving the polymer matrix electrical properties. Lee *et al.*

demonstrated the existence of torsional and tensile properties of carbon nanotube fibers-based artificial muscles subjected to different voltages [18]. It has been also demonstrated that the performance of the fibers can be improved by making yarns from the fiber mats [19]. Carbon nanotubes could modulate the matrix's properties in case of being used as fillers. Zheng *et al.* worked on polypyrrole/carbon nanotube composites and reported on improvement of the electrical conductivity, Young's modulus and tensile strength of polypyrrole when mixed with carbon nanotubes, which led to an improvement of the time variation of the response of artificial muscles [20]. The same enhancement of the properties of polymer fibers were observed when carbon nanotubes were mixed with polyaniline fibers [21]. In this case, tensile strength of 300MPa was obtained which made the resulting artificial muscles good choices for applications in which high strength is needed such as strain amplification systems and biomimetic musculoskeletal systems.

The most used ferroelectric polymers are poly(vinylidene fluoride) and its copolymers. This class of polymers has advantages over other plastics such as high dielectric constant and high flexibility which are two key parameters for designing actuators. Lu *et al.* reported on electrostrictive strains of poly(vinylidene fluoride-co-hexafluoropropylene), PVDF-HFP, and a commercial polyurethane film. Both of these types of polymers showed around 4% strain at electric field of 40MV/m [22]. Casalini *et al.* studied the effect of crosslinking on the strainof poly(vinylidene fluoride-trifluoroethylene), PVDF-TRFE. They demonstrated that crosslinking has a strong effect on actuation performance and a strain over 12% were observed at low electric field of 10 MV/m, which was much higher than that of precursors of PVDF-TRFE which was 0.70 at 20MV/m [23].

As Equation 6 suggests, the increase of the dielectric constant and polarizability of actuators represent an efficient way to improve the actuator performance. However, polymers possess a low dielectric constant typically between 2 and 12 [24]. A common method to increase the dielectric constant value of polymers, along with preserving their mechanical properties, consists of adding inorganic ceramic colloidal nanocrystals to the polymer matrix [25]. Incorporating inorganic nanofillers with high dielectric constant will lead to the formation of a new class of materials with dielectric and mechanical properties intermediate between those of the pristine ceramic and polymer materials, known as hybrid organic-inorganic nanocomposites.

## 1.3 Polymer-Ceramic Nanocomposites

Inorganic ceramic materials have special characteristics in terms of dielectric and ferroelectric properties. They show relatively a high permittivity, but they are brittle and difficult to process. The low breakdown strength is another impediment in the technological application of these materials. On the other hand, organic polymers show better mechanical properties and higher flexibility, which renders their processing much easier than that of ceramics. Although polymers possess a relatively high breakdown strength, they have a low permittivity which drastically limits their use in electronics.

Combining the properties of inorganic ceramics and organic polymers by fabricating organic-inorganic polymer-ceramic nanocomposites creates new opportunities for development of new multifunctional devices such as sensors, high voltage capacitors or electric actuators. Incorporating inorganic ceramics into the matrix of polymers yields a composite material which benefits the high dielectric constant and permittivity of ceramics and high breakdown strength

and low dielectric loss of polymers Additionally, polymer-ceramic nanocomposites retain the mechanical and thermal properties of polymers [26].

Increasing the amount of inorganic filler in a composite usually leads to an increase of the dielectric constant. However, increasing the permittivity usually results in a higher energy density and, therefore, the dielectric loss should be kept low in order to prevent the dissipation of energy, which is possible by understanding the interaction of polymer and ceramic and polymer-ceramic interface. With the recent progress in nanotechnology and new developments in the fabrication of the ceramic particles at the nanometer-length scale, the properties of the polymer-ceramic composites were substantially improved by controlling their chemical composition and morphological features. The improvement in the properties is due to the colloidal nanocrystals increase of the interface between polymer and ceramic particles whereas nanocomposites retain the innate properties of the pristine phases, in many cases product properties have been observed.

The increase of the relative permittivity of polymer-ceramic nanocomposites compared to that of the pristine polymer can be because of several factors such as change in polymer morphology at the interface, local charge distribution due to the colloidal nanocrystals surface, change in charge mobility and electron site stability [27]. These changes occur in the interface of polymer matrix and ceramic colloidal nanocrystals. Hence, controlling the interface can result in materials with higher permittivity and lower dielectric loss [26]. Currently, it is known that the polarization at interface areas is responsible for the majority of the dielectric loss [27]. Hence, controlling the interface of the polymer-ceramic nanocomposites can improve these nanocomposites properties such as energy storage capacity.

## 1.4 Nanofibers

With the development of nanotechnology, various shapes of nanomaterials with different dimensions have been fabricated. These shapes include 0-dimensional (0-D) nanomaterials, which all dimensions are in the scale of nanometer (= $10^{-9}$ meter), such as colloidal nanocrystals, 1-D nanomaterials, which consist of one dimension in macroscale and two in nanoscale, such as nanotubes or nanorods, and 2-D nanomaterials which have two dimensions in macroscale and one in nanoscale, such as nanosheets. Among these shapes, nanofibers showed interesting properties. Nanofibers include features such as pores with controllable morphology, high degree of porosity and high specific surface area. Nanofibers are defined as fibers with diameters less than 100 nm. But nowadays fibers with diameters less than 1000nm are called nanofibers.

A wide range of materials, including various types of polymers and ceramics have been used in the fabrication of nanofibers [28, 29]. The latter one made them to be used for various technological applications. Tissue engineering, drug delivery, cell delivery, organ implants in the medical field, fuel cells, solar cells, batteries in energy storage and conversion sensors (nano and bio sensors), catalysis, filtration and textile manufacturing are only a few examples of the technological applications.

Various methods have been developed for the fabrication of nanofibers, such as drawing, template synthesis, phase separation, self-assembly and electrospinning [30]. Electrospinning is known as the most common way for making nanofibers.

## 1.5 The Electrospinning Method

Electrospinning is the process of drawing fibers from a solution with certain viscoelasticity on a conductive substrate by using electrostatic force. Electrospinning is known as

the best method for fabricating nanofibers with the desired morphology. The ease of use and low-cost apparatus made this method the most favored way for making nanofibers. This process was first patented by John Francis Cooley in 1900 [31]. John Zeleny was the first to start working on mathematically modeling fluid behavior under electrostatic forces and published his works in 1914 [32]. Anton Formahls contributed a lot to progress of electrospinning by publishing numerous patents between 1931 and 1944 [33].

Extensive work has been done on electrospinning during the past100 years in order to understand the fundamentals of this field and to predict and control this process. During the last 30 years, fibers with different morphology have been fabricated for a wide range of applications such as drug delivery systems, tissue engineering, energy storage devices and filtration.

## 1.6 The Electrospinning Process and the Parameters Affecting it

In order to be able to draw fiber from solution, the solution should have certain degrees of viscoelasticity. Hence polymers are the best choice for fiber materials. Electrospinning apparatus as shown in Figure 3 consists of:

- High voltage supplier and electrodes
- A nozzle (usually a syringe and metal needle)
- Pump to maintain a constant flow rate
- Conductive substrate or collector

As shown in Figure 3, an electrode is connected to the needle and the other one is attached to the collector, making the collector and needle oppositely charged. The solution is pumped out with constant flow rate, the solvent would evaporate off in the distance between the needle and collector and what remain in the substrate would be polymeric fibers.

In this process 3 factors are considered:

- The diameter of fibers should be uniform and controllable
- Surface of fibers be defect free or defect controllable and
- Continuous nanofibers can be produced

In order to meet the above requirements, many parameters should be controlled.

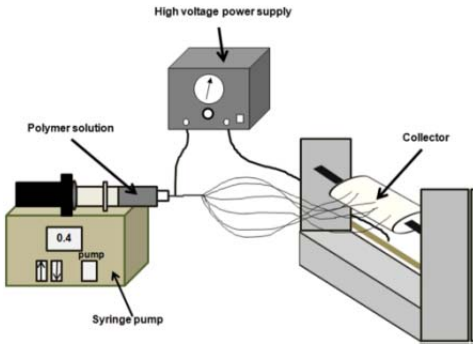

Figure 3. Electrospinning apparatus

The choice of the solvent is critical. The solvent should have enough volatility to evaporate off in the distance between the needle tip and the collector. Polar solvents are typically better choices and they can increase the charge on the surface of the solution due to their high dielectric constants, resulting in a more efficient electrospinning. In addition to the solvent, concentration of the polymer in the solution is another key factor for electrospinning. In which, increasing the polymer concentration results in fibers with higher diameters but bead free [36]. The electrospinning condition parameters play an important role in this process as well, which in order to obtain thinner fibers, increasing the electric field or lowering the flow rate may be utilized.

## 1.7 Technological Applications of Nanofibers

Numerous applications in different fields have been proposed for polymer nanofibers. In this section some of the applications are introduced and reviewed in brief. In the medical field, polymer nanofibers have found applications in drug delivery, tissue engineering, wound dressing and artificial organs or implants. Biodegradable polymers are top choices for using in biomedical applications. Khademhosseini *et al*. [37] reported the use of nanofibers in tissue engineering. They used electrospinning for turning biodegradable polymers into nanofibers for making scaffolds and replace or bypass the damaged arteries in various cardiovascular diseases. Kenawy *et al.* [38] work on drug delivery systems based on the electrospun nanofibers is another example of the application of these materials in biomedical applications. They fabricated nanofibers from poly(lactic acid) and poly(ethylene-co-vinylacetate) and after incorporating tetracycline as drug, in the fiber mats, studied the release behavior of these systems.

Polymer nanofibers can also be used in electronics. Piezoelectric sensors have been made from poly(vinylidene fluoride) nanofibers [39]. Persano *et al*. [40] developed high performance piezoelectric devices for pressure/force sensors and mechanical energy harvesters based poly(vinylidene fluoride) nanofibers. Other applications of these materials in this field such as field effective transistors, ion electrolyte gate devices and semiconductors were reviewed by Luzio *et al.* [41]. The use of nanofibers in energy related applications has been studied in literature numerously. They have been widely used as electrolytes in solar cells, in particular after the introduction of solid state solar cells [42, 43]. Wang *et. al.* studied the applications of flexible nanofibers in energy storage applications and discussed their performance as supercapacitors and lithium-ion batteries [44]. More recent applications of nanofibers in this field are related to electric actuators and artificial muscles. Carbon nanotube yarns and

conductive polymers such as polyaniline were examined for this purpose and their deformation in the electric field was measured [18, 21].

# CHAPTER II

# MATERIALS AND METHODS

In order to make polymer-ceramics fibers, two components of organic and inorganic phase were mixed. In this work, poly(vinylidene fluoride *co*-hexafluoropropylene) (PVDF-HFP) was selected as organic phase and inorganic BaTiO3 colloidal nanocrystals were incorporated into the polymer matrix.

## 2.1 Poly(vinylidene fluoride), PVDF and the PVDF copolymers

Poly(vinylidene fluoride) or PVDF is a thermoplastic fluoropolymer which is produced by emulsion polymerization of vinyledene difluoride (1,1-difluoroethylene). This polymer is recognized for its toughness and special electrical properties such as high dielectric constant. The electrical properties, mostly originate from the polarity of alternating groups of $CH_2$ and $CF_2$ on the polymer chain backbone. PVDF structure is demonstrated in Figure 4.

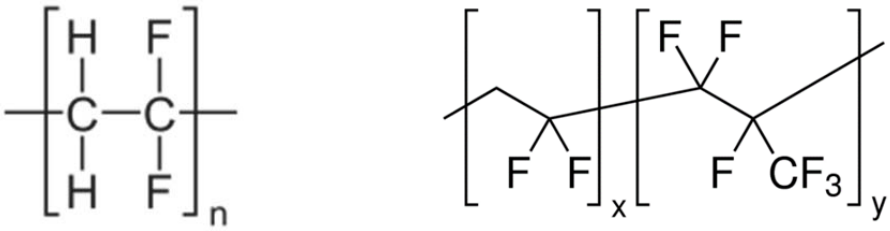


Figure 4. PVDF and PVDF-HFP structures

PVDF has shown ferroelectricity, piezoelectricity and pyroelectricity under certain circumstances. For showing those properties, it should be mechanically stretched and then poled under tension to align the dipoles in the crystalline PVDF structure. PVDF consists of at least five structural conformations depending on the trans (T) or gauche (G) linkages in the polymer chain backbone. The most abundant form which is seen in the bulk structure is alpha ($\alpha$) phase

and is made of TGTG conformation and by aligning the dipoles, beta ($\beta$) phase is obtained which is responsible for the ferroelectric properties and has the conformation of TTTT [45]. Figure 5 illustrates the alpha and beta phase structure.

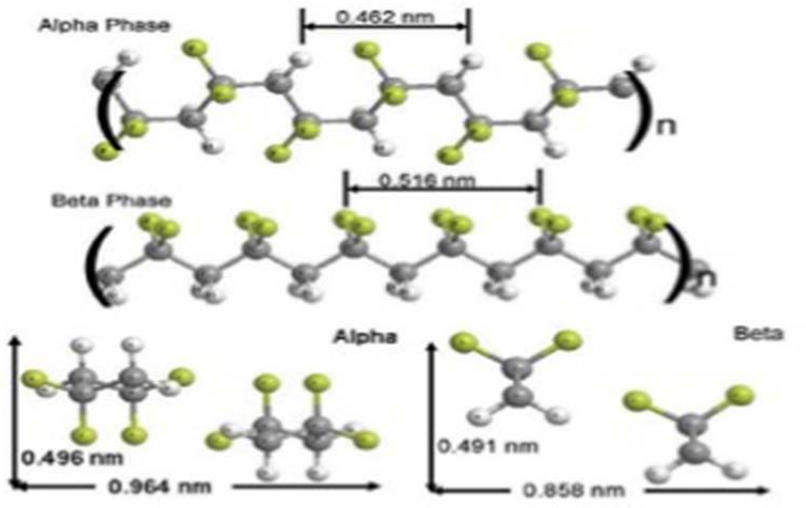


Figure 5. Alpha and beta conformation in PVDF structure [2]

Copolymers of PVDF with other fluorinated species are produced for modifying the properties of this polymer. The most common copolymers are poly(vinylidene fluoride *co*-hexafluoropropylene) or PVDF-HFP and poly(vinylidene fluoride co-trifluoroethylene) or PVDF-trfe, which flexibility and dielectric properties was increased in each copolymer, respectively.

This family of polymers have been widely used for different type applications such as coatings, metal paints and membranes because of their special properties such as flexibility, low weight and high chemical corrosion resistance. But they are mostly known for their high dielectric constant and ferroelectric proprieties and have been used in electronics as sensors, piezoelectric devices, energy storage devices, capacitors, transistors and etc [46-51].

## 2.2 $BaTiO_3$, an Archetypal Ferroelectric Ceramic

BaTiO3 is a ceramic with perovskite crystalline structure with the general formula of $BaTiO_3$. This ceramic shows interesting electrical properties including ferroelectricity and high dielectric constant which have made it a proper candidate for applications such as memory and high energy density storage devices, semiconductors and organic-inorganic hybrid capacitors. The general formula of perovskite is $ABX_3$ and these materials possess a crystal structure in which the "A" cation is in the corner of the cube, the "B" cation is in the center of the cube and the "X" anion is in the center of the face edges (Figure 6).

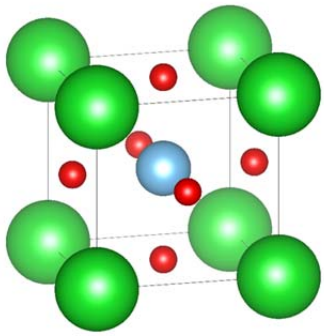

Figure 6. Cubic structure of $BaTiO_3$ as a perovskite

The value of the dielectric constant depends on various parameters such as the synthesis route, temperature, dopants and measurement conditions. Hence, the purity, shape and grain size of the $BaTiO_3$ can affect their performance.

# CHAPTER III

# EXPERIMENTAL SECTION

## 3.1 Sample Preparation

Polymer solutions were prepared by dissolving PVDF-HFP pellets (Mw~470000, Aldrich) in the N,N-dimethylformamide (DMF) and acetone mixture as the solvent. The surface of the barium titanate ($BaTiO_3$) colloidal nanocrystals with oleic acid ligands were modified to make them dispersible in polar solutions. 5 mmol of $BaTiO_3$ colloidal nanocrystals in hexane were mixed with 5 ml of nitrosonium tetrafluoroborate ($NOBF_4$) in DMF solutions. The resulting mixture was stirred until the $BaTiO_3$ colloidal nanocrystals transferred from hexane into DMF through the interface between the polar and nonpolar phases. The $BaTiO_3$ colloidal nanocrystals with ionic ligands were added to the PVDF-HFP solutions to prepare solutions with different $BaTiO_3$/PVDF-HFP concentration of 0, 2 and 4 wt%. The PVDF-HFP concentration was kept at 14 wt% in all solutions, while DMF/acetone weight ratio was kept 7:3. Although, DMF was a proper polar solvent to dissolve the polymer-ceramic mixture, acetone as a volatile solvent was used to ease the electrospinning process.

Electrospinning was carried out using the prepared solutions. An aluminum foil was used as the collector. The needle tip to collector distance was chosen to 15 cm, the applied voltage was 19 KV and the flow rate was kept to 0.1 ml/hr. The nanofibers mats were peeled off from the collector to be used for characterization.

## 3.2 Structural Characterization

The structure and morphology of electrospun polymer-ceramic fibers were studied and characterized by Hitachi S-3400N scanning electron microscopy (SEM), Asylum Research MFP-

3D atomic force microscopy (AFM) using a standard tip AC240TS-R3 and a Rigaku MiniFlex II X-ray diffractometer for X-ray diffraction (XRD). Philips CM10 transmission electron microscopy (TEM) was used to capture images of BTO colloidal nanocrystals. Conformational structure of nanofibers was studied using a Nicolet iS50 ATR, Thermo Scientific Fourier transform infrared spectroscopy (FTIR). Thermal analysis of fiber samples was carried out by differential scanning calorimetry (DSC) using a TA Q2000 instrument using a ramp heating rate of 5 $℃/min$ at nitrogen atmosphere.

### 3.3 Mechanical Properties

The Mechanical properties of polymer-ceramic fibers were measured using a TA Q800 instrument. Fiber mats were cut into ribbons and mounted in the instrument. The stress-strain curve was obtained in a strain ramp mode with a rate of 10 %/min at room temperature.

### 3.4 Dielectric Measurements

The dielectric properties of polymer-ceramic nanocomposites were measured using Agilant 4294A Precision impedance analyzer at room temperature. Films of PVDF-HFP/$BaTiO_3$ nanocomposites were cast on glass substrates with the same solution used for electrospinning. Electrodes of Gold and Palladium (Au/Pd) with the thickness of 100nm and an area of 0.28 $cm^2$ were deposited on the both sides of the films using a Denton sputter coater to make parallel plate capacitors. The same samples were used for studying the polarization in the films using a Radiant Technologies Inc, Precision Premier II ferroelectric tester by obtaining the hysteresis loop.

3.5 Electromechanical Characterization

In order to study the electromechanical properties of polymer-ceramic fibers, mats were cut into strips of 2x3.25 cm. Electrodes were deposited on the PVDF-HFP/$BaTiO_3$ strips. The area of electrodes was 1.5x3 cm. The electrostrictive strain of the nanocomposite fibers has been measured by using an air gap capacitor. The capacitance of the air gap capacitor was measured with HP 4284A impedance analyzer. The change in capacitance then was related to the change in thickness of the nanocomposite fiber strips. The setup is shown in Figure 6.

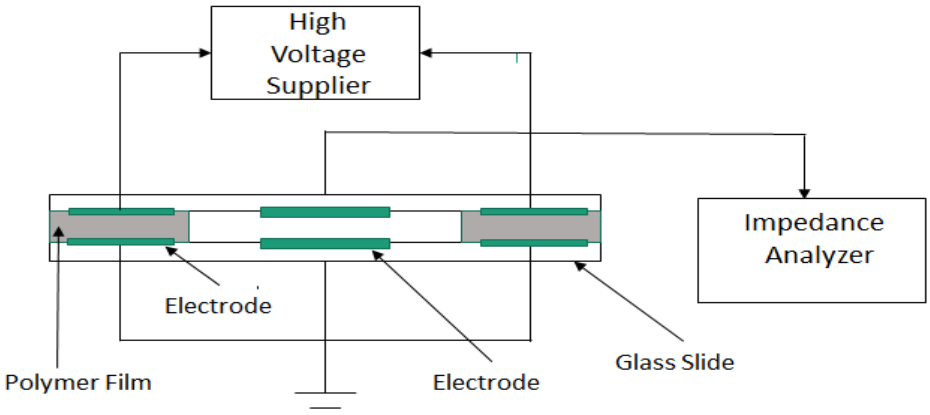


Figure 7. The setup which was used for actuation tensile measurement, with labeled components

# CHAPTER IV

## RESULTS AND DISCUSSION

Interaction between polymer chains and ceramic colloidal nanocrystals plays an important role in the properties of the resulting polymer-ceramic nanocomposites. In this work, $BaTiO_3$ was chosen as a filler and PVDF-HFP as the matrix. A challenge associated with polymer-ceramic nanocomposite systems is the proper dispersion of the ceramic colloidal nanocrystals into the polymer matrix and preventing the aggregation of colloidal nanocrystals [52]. Therefore, the surface of the inorganic colloidal nanocrystals should be modified in the way which increases the compatibility between the particles and polymer chains. The colloidal nanocrystals used in this work were synthesized in the way that they were covered by non-polar molecules of oleic acid, which typically were not miscible with polar compounds or dispersible in polar solvents. In order to increase the polarity of the colloidal nanocrystals and make them similar to that of the polymer, the ligands should be replaced by polar groups. Parizi *et al.* reported on a method based on using $NOBF_4$ as reagents for switching the ligands on the surface of $BaTiO_3$ nanocube crystals [52]. The same method was utilized here to increase the miscibility of the $BaTiO_3$ colloidal nanocrystals and PVDF-HFP. This process is simple and happens fast which results in high dispersion of $BaTiO_3$ colloidal nanocrystals in DMF. Figure 7 shows the $BaTiO_3$ nanocubes with ligands before and after the ligand exchange.

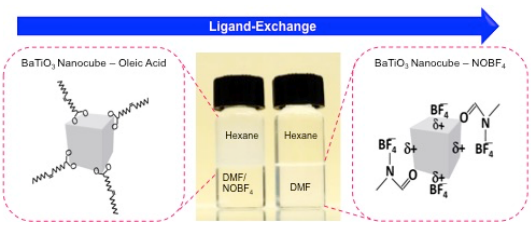


Figure 8. $BaTiO_3$ cubic colloidal nanocrystals before and after the surface modification with ionic $NOBF_4$ [52]

4.1 Structural Characterization

The electrospinning of the solutions was done at high voltage of 19 kv and a constant flow rate of 0.1 ml/hr, while the needle tip to collector distance was kept at 15 cm. High voltage was used to reduce the fibers diameters and fabricate fibers with diameter in nanometers scale. The SEM images of the samples suggested nanofibers with the diameter range of 200-400 nm were collected with a scanning electron microscope. It is worth noting that the addition of ceramic nanofibers did not affect the size of majority of nanofibers although, some thinner strings, with diameters ranging between 100-200 nm, in sample with 4% $BaTiO_3$ compared to that of polymer nanofibers were observed. This can be explained by the higher amount of colloidal nanocrystals and ionic $NOBF_4$ ligands in the solution which increased the charge and the turbulence on the solution surface.

Figures 8 and 9 show the SEM images of the nanofibers and the TEM images of $BaTiO_3$ colloidal nanocrystals. The $BaTiO_3$ colloidal nanocrystals nanocubes used in this experiment have an average edge length of 15 nm The nanocomposite fiber mats made by electrospinning were porous and their surface was relatively rough based upon the AFM images.

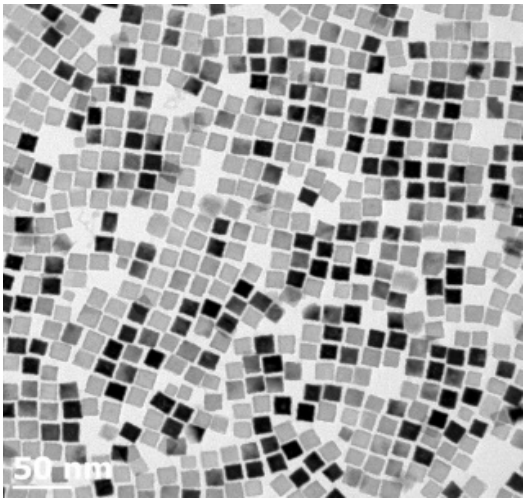

Figure 9. TEM picture of $BaTiO_3$ nanocubes

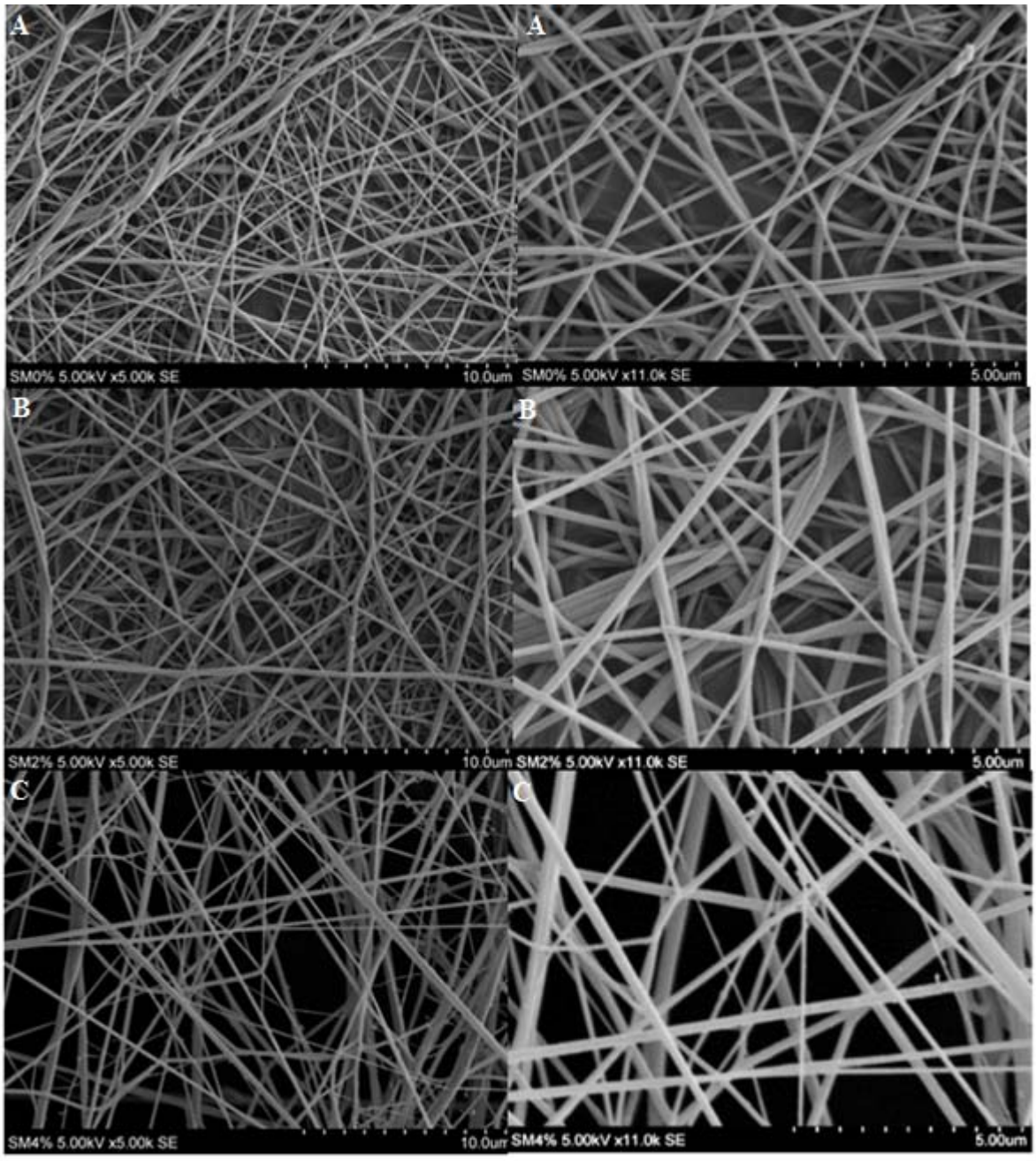


Figure 10. SEM images of PVDF-HFP nanofibers ithout and with $BaTiO_3$ colloidal nanocrystals. A) Electrospun PVDF-HFP nanofibers B) Electrospun PVDF-HFP nanocomposite fibers with 2wt% $BaTiO_3$ C) Electrospun PVDF-HFP nanocomposite fibers containing 4wt% $BaTiO_3$

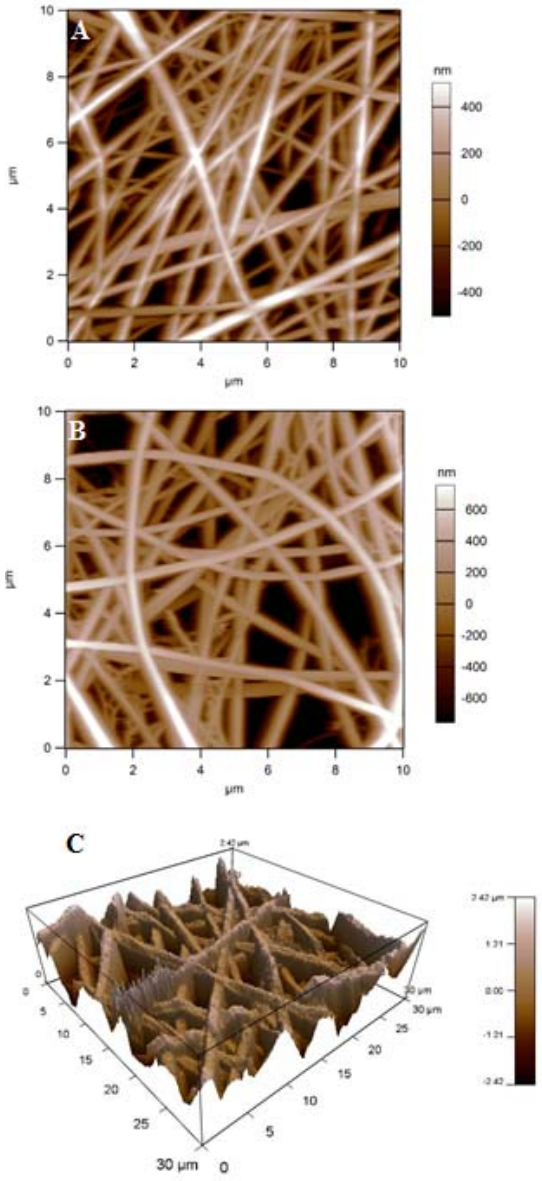


Figure 11. Atomic force microscopy (AFM) images of PVDF-HFP nanofibers showing the morphology of the fibers and the porosity of fiber mats in the absence and the presence of $BaTiO_3$ colloidal nanocrystals. A) Electrospun PVDF-HFP nanofibers. B) Electrospun PVDF-HFP with 4 wt% $BaTiO_3$. C) SEM image showing the topography of fiber mats

The FTIR spectrum of the sample indicated the formation of both $\alpha$ and β- phase in the structure of all nanofiber samples. The peaks at 530 $cm^{-1}$ and 840 $cm^{-1}$ correspond to $\alpha$ and β-phase , respectively. The formation of β- phase introduce crystalline regions into the structure of

nanofibers. This crystallization is related to alignment of the fluorine groups alongside each other.

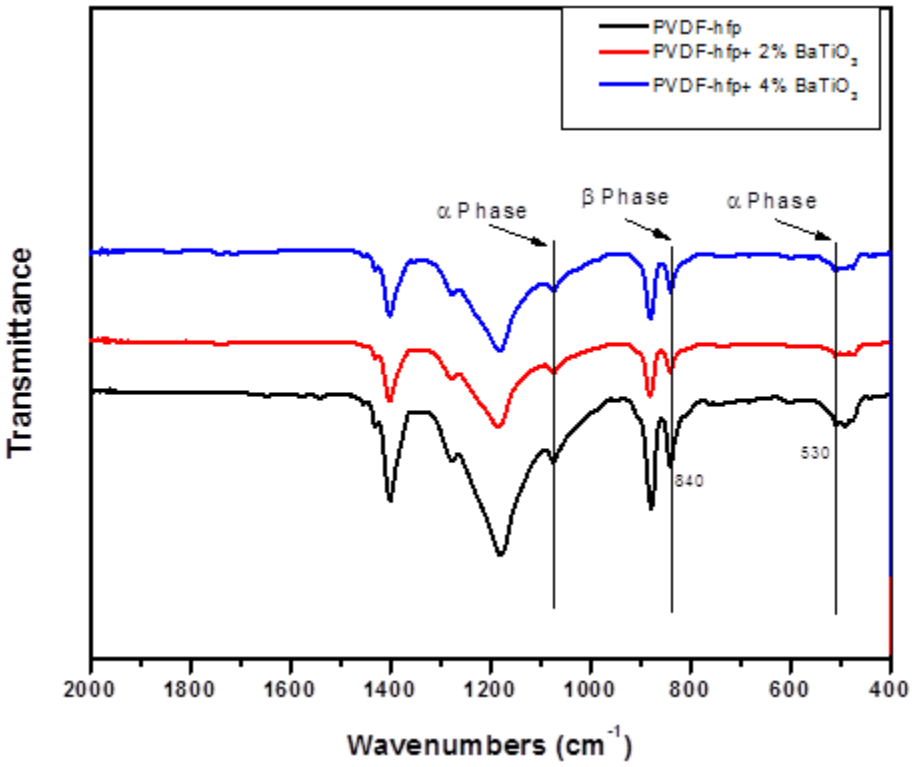


Figure 12. FTIR spectra of samples showing different phases in the nanofibers

The XRD experiment showed the crystalline structure of the both nanocomposite fibers and $BaTiO_3$ colloidal nanocrystals. The broad peak at 21° in 2 θ corresponds to the β- phase in the PVDF-HFP structure. The broadness of this peak showed the low crystallinity in the samples. Another peak was seen at 18° in 2 θ which was related to the $\alpha$ phase in PVDF-HFP matrix. The peak at 31° in 2 θ in $BaTiO_3$ is the 110 plane, which also is the characteristic peak and the presence of this peak in nanocomposite samples showed the incorporation of the $BaTiO_3$ colloidal nanocrystals in the structure of the polymeric nanofibers. This peak was even more

pronounced by increasing the content of the $BaTiO_3$ cuboidal colloidal nanocrystals in the samples.

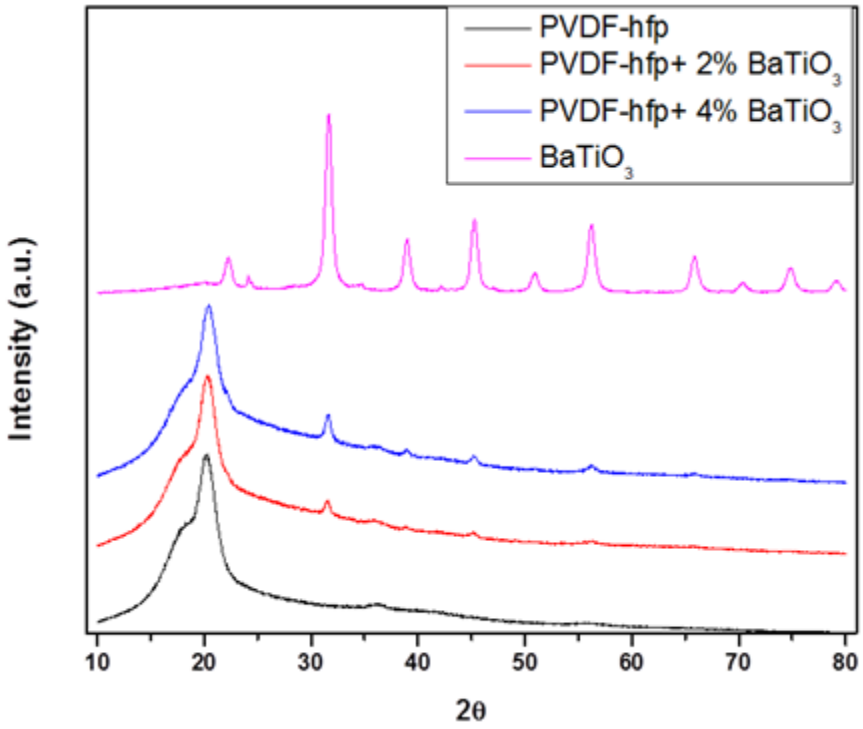


Figure 13. X-ray diffraction (XRD) spectrum of samples showing the crystalline structure of each one

Differential scanning calorimetry (DSC) was used to study the thermal transitions in the nanocomposite fibers. The exothermic peaks between 110 ℃ and 150 ℃ correspond to the melting process. The melting point of PVDF-HFP nanofiber did not have noticeable change and a melting point of 130 ℃ was seen in all samples. The XRD results and DSC results both suggested some degree of crystallization in the sample, which the crystallization was quantified using DSC.

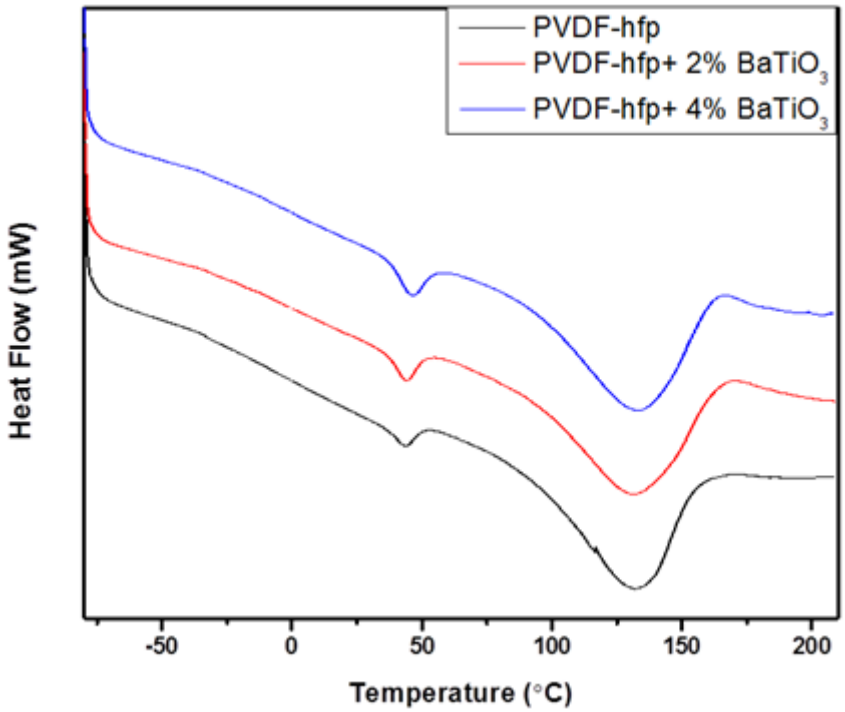

Figure 14. Differential scanning calorimetry (DSC) of polymer-ceramic nanocomposites

The percent crystallization of each sample was obtained by calculating the area of the melting peak. The reported enthalpy of fully crystalline PVDF is $\Delta H$= 104.5 J/g. The DSC data for the as spun nanocomposite fibers is shown in Table1. A degree of crystallinity varying between 20 and 30% was found in all samples. It should be noted that adding $BaTiO_3$ colloidal nanocrystals could increase the crystallinity with a very small amount; that is from 22.5% in pristine polymer nanofibers to 27.9% and 25.5% for nanocomposite fibers with 2% and 4% $BaTiO_3$, respectively.

Table 1. Data corresponding to crystallinity of each sample based on DSC, showing the percent crystallinity about 30% for each sample

| Sample | Ref. | PVDF-HFP | PVDF-HFP+ 2%$BaTiO_3$ | PVDF-HFP+ 4%$BaTiO_3$ |
|---|---|---|---|---|
| $\Delta H$ (J/g) | 104.5 | 23.15 | 29.19 | 26.71 |
| %Crystallinity | 100 | 22.5 | 27.9 | 25.5 |

4.2 Dynamic Mechanical Analysis

In general, addition of ceramic fillers to polymer matrix leads to an increase of the stiffness and the strength of the polymer host matrix. Figure 8 shows the stress-strain curve for PVDF-HFP nanofibers and PVDF-HFP/$BaTiO_3$ nanofiber composites. As expected, the Young modulus increased by increasing the concentration of nanofiller in the sample. The measured Young's modulus values of the samples were 9.2 MPa, 20.3 MPa and 24.9 MPa for PVDF-HFP nanofibers, nanocomposite fibers with 2% $BaTiO_3$ and 4% $BaTiO_3$, respectively. The PVDF-HFP nanofibers showed high flexibility and strain to failure for the polymer nanofiber were more than 200%, which was higher than that of the sample with 2% $BaTiO_3$ which was 130%. The strain to failure for sample with 4% $BaTiO_3$ almost halved compared to PVDF-HFP nanofibers and reached 90% in these samples. Unlike the strain, the strength to failure was increased by addition of ceramic filler and the measured values were almost two times higher for samples with 2% and 4% $BaTiO_3$, respectively compared to the strength of polymer nanofibers. Although the increase of the stiffness is not favorable for actuation, the nanocomposite fibers still show proper flexibility and strength suitable for use in artificial muscle applications. Table 2 summarizes the experimental DMA results.

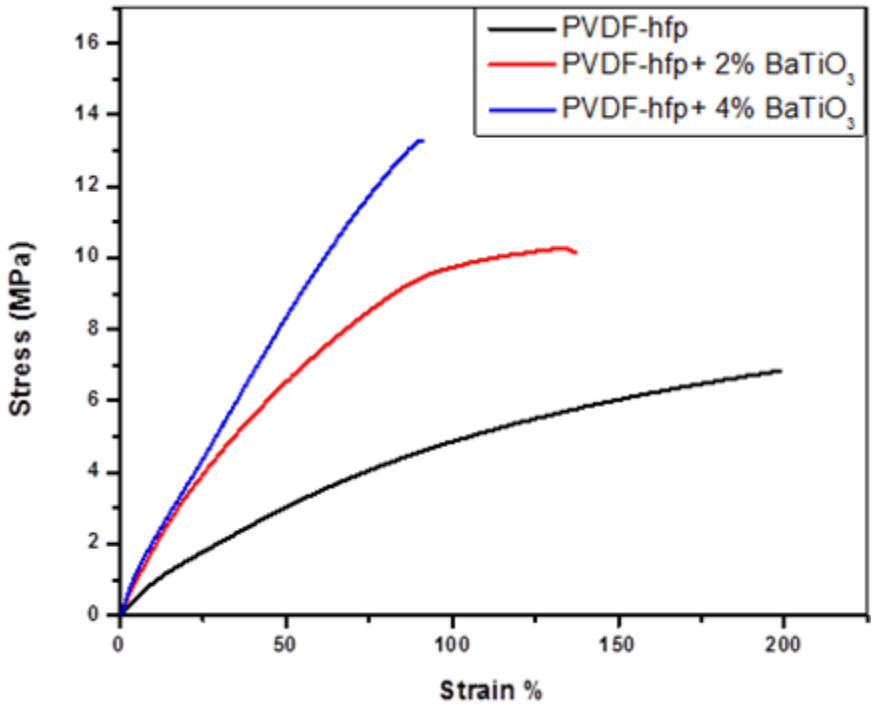


Figure 15. Dynamic mechanical analysis (DMA) of the nanofibers, showing the increase in strength and Young's modulus by increasing the $BaTiO_3$ content

Table 2. Summary of the important data obtained by dynamic mechanical analysis (DMA)

| Samples | PVDF-HFP | PVDF-HFP+ 2%$BaTiO_3$ | PVDF-HFP+ 4%$BaTiO_3$ |
|---|---|---|---|
| Maximum Strain (%) | 198 | 137 | 91 |
| Maximum Stress (MPa) | 6.8 | 10.3 | 13.2 |
| Young's Modulus (MPa) | 9.2 | 20.3 | 24.9 |

The mechanical properties are highly dependent on the interaction between the polymer chains and the filler particles in polymer-ceramic nanocomposites. Ionic ligands of $BF_4^-$ passivating the surface of the $BaTiO_3$ nanocrystals could not only improve the distribution of colloidal nanocrystals on the polymer matrix, but also increase the interaction between the polymer chains and particles [1]. It has been stated that the addition of colloidal nanocrystals can

restrict the motion of polymer chain and results in a stiffer material [53, 54]. As a result, PVDF-HFP/$BaTiO_3$ nanocomposite fibers showed a lower strain to failure compared to that of PVDF-HFP nanofibers, showing a higher stiffness in the nanocomposite samples.

## 4.3 Dielectric Spectroscopy of Fibrous Materials

Fiber mats made by electrospinning were collected by a conductive substrate, aluminum foil. The mats were porous and consisted of randomly oriented fibers. Measuring dielectric constant of fiber mats cannot be accurate. Hence, the films have been cast for this purpose and compared to show the effect of the addition of the BaTiO3 nanofiller on the relative permittivity of the samples. As seen in Figure 14, the relative permittivity of the PVDF-HFP/$BaTiO_3$ systems reached a maximum of $\varepsilon = 16$ at a frequency of 1 KHz, value which was higher than that of neat PVDF-HFP ($\varepsilon = 11$). The obtained experimental results illustrated the decrease with the frequency because of the lower mobility of electrical dipoles in high frequency region. Although the values are not the same for the nanofibers, they demonstrate that the addition of the inorganic nanofillers to the sample enhances the relative permittivity of the polymer matrix. Hence, the relative permittivity should be improved in the PVDF-HFP/$BaTiO_3$ nanocomposite fibers as well.

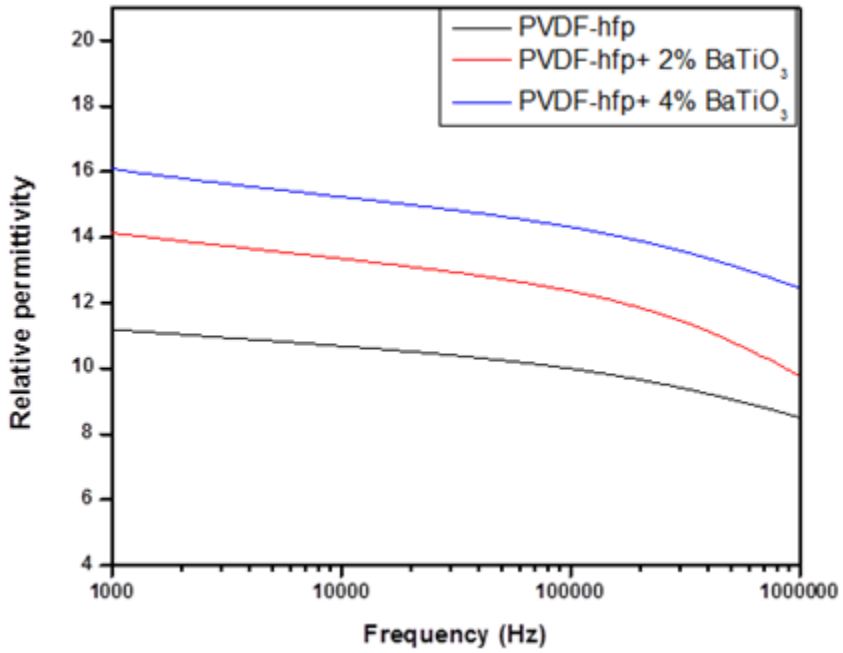

Figure 16. Dielectric spectroscopy of polymer and polymer-ceramic films

The increase of the dielectric permittivity is generally expected in nanocomposites and this improvement in the dielectric properties of polymer-ceramic nanocomposites compared to the pure polymer can be ascribed to numerous factors, such as change in polymer morphology at the interface, local charge distribution due to the colloidal nanocrystals surface, change in charge mobility and electron site stability [27].

The dielectric loss was also measured for the of polymer-ceramic fibers with various content of dielectric filler. This parameter shows the dissipated energy through dielectric spectroscopy measurements and, by definition, is the loss of energy due to the movement of charges when the polarization switches direction. The dielectric loss is generally affected by different parameters, such as direct current conduction, space charge migration and the relaxation of dipole. Although the loss factor does not provide useful information about the performance of artificial muscles, low values indicated a low waste of energy in the dielectric spectroscopy test.

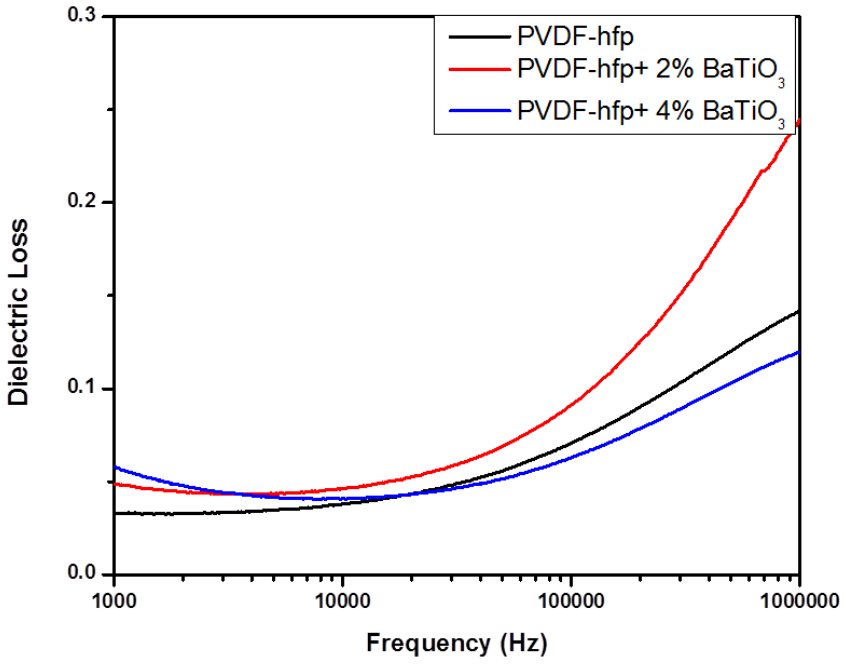


Figure 17. Dielectric loss of samples

4.4 The Electric Hysteresis Loop

The actuation tensile is highly dependent on the polarization of the samples in the electric field and how dipoles are oriented in the samples. The polarization in nanofibers is very difficult to obtain due to the same reason as dielectric constant measurement conditions. Thus, the same films were used for predicting the polarization in the PVDF-HFP/$BaTiO_3$ nanocomposites. Figure 11 illustrates the polarization in films. As predicted, the polarization increased by addition of $BaTiO_3$ colloidal nanocrystals. The increase in polarization can be defined by the fact that dipoles in $BaTiO_3$ colloidal nanocrystals can polarize in an easier manner than that of polymer. Hence, higher polarization was seen in nanocomposite samples. The dielectric measurement and hysteresis loop showed a higher dielectric constant and polarization in nanocomposites compared to those of the pristine polymer. As a result, a higher actuation tensile is expected to be seen in the polymer-fiber structures when subjected to the action of an external electric field.

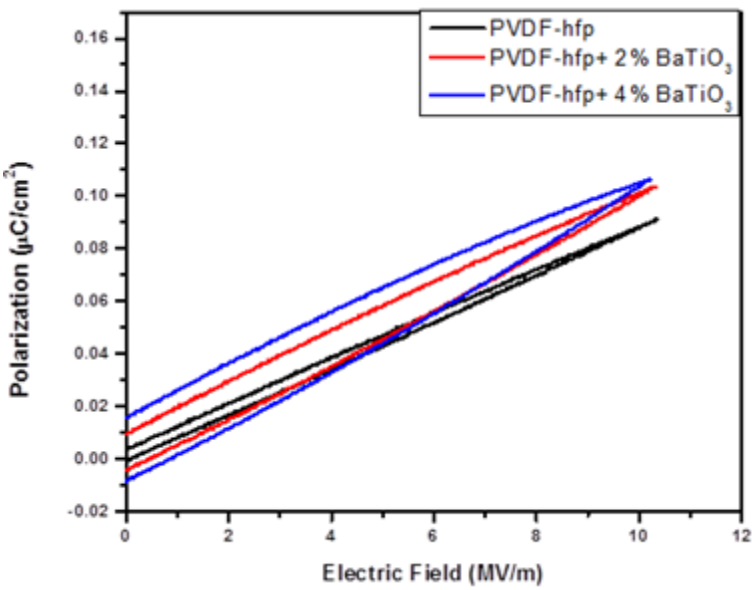


Figure 18. Electric hysteresis loop of the polymer and the nanocomposite samples

4.5 The Electromechanical Response and the Actuation Tensile

The electrostrictive strain at a relatively low electric field (up to10 MV/m) were measured using an air gap capacitor connected to an impedance analyzer. Two fiber mat strips were cut in size of 2x3.25 cm and electrodes of Au/Pd were deposited on the samples. One side of the electrodes was connected to a voltage supplier and the other side was grounded. By applying the voltage to the sample strips, the capacitance of the air gap capacitor was measured and the change in capacitance was related to the change in thickness by the capacitance e equation:

$$C = \varepsilon_0 A/z \quad => \quad z = \varepsilon_0 A/C \quad \text{Eq. (8)}$$

where $\varepsilon_0$ is the permittivity of the air, $A$ is the area of the air gap capacitor and $C$ is the capacitance of the air gap capacitor. Since the samples were sandwiched between the glass slides, the thickness of the air gap capacitor equals with the thickness of the samples. Hence, applying voltage on the samples could cause a strain in the samples in the direction of electric

field and as a result, will reduce the thickness and change the capacitance of air gap capacitor (Figure 19). The change in strain in the direction of electric field (thickness of the samples) was calculated as a function of the electric field and is shown in Figure 20.

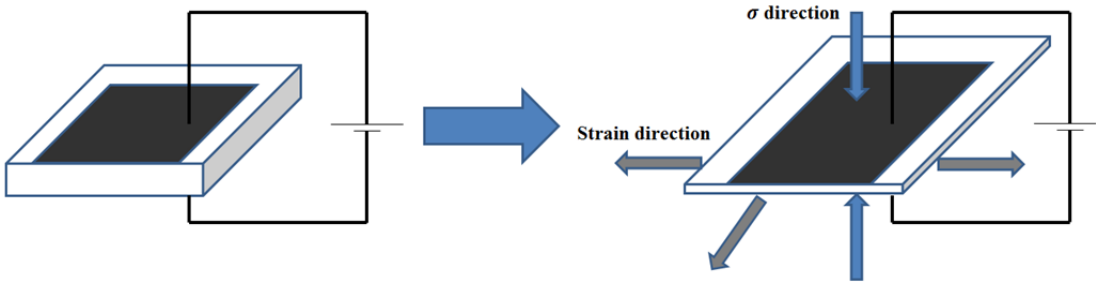


Figure 19. Demonstration of strips used for actuation tensile measurement. Left image shows the sample in absence of electric field and right image is the sample in the electric field undergoing actuation which will result in an increase in area and a decrease in thickness

The PVDF-HFP nanofibers exhibited maximum strains about 1.1% at 10 MV/m, which agrees well with what already was reported for PVDF-HFP films by Lu *et al*. [22]. Strains for nanocomposite fibers containing 2% $BaTiO_3$ was measured about 2%. The highest actuation response observed in the sample with 4% $BaTiO_3$ which was more than 3 times higher than that of the pristine polymer.

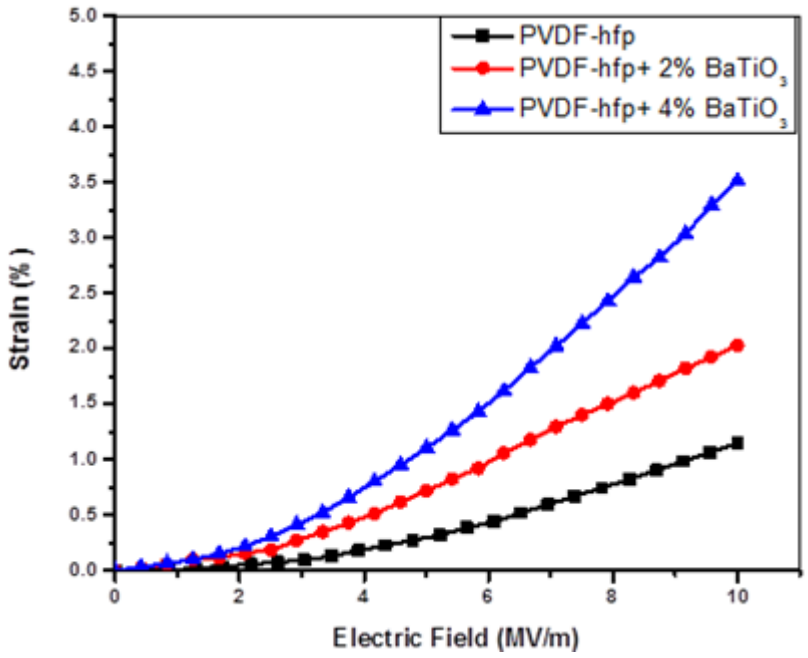

Figure 20. Actuation tensile of electrospun nanofiber mats in a low electric field of up to 10MV/m and in the direction of the electric field or thickness of the sample

The increase of the strain in nanocomposite fibers can be related to the presence of $BaTiO_3$ colloidal nanocrystals and their effect on increasing the dielectric constant and finally polarization in the applied electric field. The PVDF-HFP molecules are highly polar because of the difference in electronegativity between the fluorine and and the carbon atoms in the chain structure. Dipoles can be aligned to the direction of the electric field and undergo a small displacement in the electric field, which this will result in a strain. The polarization would even increase more after addition of $BaTiO_3$ colloidal nanocrystals thus, an increase in the electrostrictive strains of nanocomposite samples can be observed.

# CHAPTER V

# CONCLUSIONS

In this work, electric actuators made from PVDF-HFP nanofibers and PVDF-HFP/$BaTiO_3$ nanocomposite fibers were fabricated and their performance as artificial muscles and the effect of the addition of $BaTiO_3$ nanoparticles to the polymer matrix, as an effective way to improve the artificial muscle performance, were studied. A relatively concentration of the inorganic fillers was used in order to retain the flexibility of polymer fibers and avoid the aggregation of the colloidal nanocrystals. The average diameter of the electrospun nanofibers diameter varied between 200 and 400 nm and the DSC results suggested that the crystallinity of the samples varied between 22% and 28% Addition of the $BaTiO_3$ colloidal nanocrystals to the polymer matrix have a substantial impact on the performance of the nanofibers as artificial muscles. As expected, the stiffness of the fibers increased upon increasing the content of the $BaTiO_3$ nanoparticles. Additionally, the electromechanical tests indicated an increase of more than 3 times of the actuation strain of the nanocomposite fibers containing 4% $BaTiO_3$ nanoparticles compared to that of pristine polymer nanofibers under electric fields as low as of 10MV/m. The fabricated artificial muscles can potentially be used in applications which require electric actuation performance such as medical devices, robotic systems and microfluidic pumps, as well as toys.

# CHAPTER VI

# FUTURE WORKS

In this work artificial muscles were made from poly(vinylidene fluoride co-hexafluoropropylene) nanofiber mats and reinforced with $BaTiO_3$ colloidal nanocrystals to modulate their properties. In order to have a more versatile analysis of these systems and to fabricate artificial muscles with improved performance, one can study different parameters involving in the nature of colloidal nanocrystals, structure of polymers and measurement modes of actuation.

By twisting a ribbon of fiber mats, yarns are made which have higher mechanical properties in terms of strength and strain to failure compared to those of mats. These parameters can even be strengthened by twisting the yarns and forming coils. These coils undergo strains up to 700% [55], which can mimic the real muscles structure in a more similar way and will lead to the formation of high strength artificial muscles.

The nature of the inorganic fillers and their interaction with polymer chains can be another topic of interest. The aspect ratio can play an important role in the properties of materials such as tensile and electrical properties. It is predicted that using colloidal nanocrystals with higher aspect ratios such as nanotubes or nanoarrays can change the performance of the fabricated polymer-ceramic nanofibers, since they possess higher dielectric constant. Also, other fillers with different dielectric properties and stiffness such as titanium dioxide ($TiO_2$) and lead zirconate titanate (PZT) can be used in making polymer-ceramic artificial muscles and the performance of artificial muscles with different fillers be compared.

Applying the electric field may cause stimulation in the sample and create a mechanical torque. The mechanical torque can be in form of contraction, expansion, rotation and etc.

Response time and reversibility of the deformation are two other important parameters for designing an actuator for a specific application. In this work only contraction in fibers was studied. Hence, studying other types of actuations and response times of artificial muscles can be other ways to evaluate their efficiency and performance.

REFERENCES


1. Stoyanov, Hristiyan, Matthias Kollosche, Sebastian Risse, Denis N. McCarthy, and Guggi Kofod. "Elastic block copolymer nanocomposites with controlled interfacial interactions for artificial muscles with direct voltage control." *Soft Matter* 7, no. 1 (2011): 194-202.
2. Mirfakhrai, Tissaphern, John DW Madden, and Ray H. Baughman. "Polymer artificial muscles." *Materials today* 10, no. 4 (2007): 30-38.
3. Huang, Cheng, R. Klein, Feng Xia, Hengfeng Li, Q. M. Zhang, François Bauer, and Z. Y. Cheng. "Poly (vinylidene fluoride-trifluoroethylene) based high performance electroactive polymers." *Dielectrics and Electrical Insulation, IEEE Transactions on* 11, no. 2 (2004): 299-311.
4. Zhao, Xuanhe, and Zhigang Suo. "Electrostriction in elastic dielectrics undergoing large deformation." *Journal of Applied Physics* 104, no. 12 (2008): 123530.
5. Pelrine, Ronald E., Roy D. Kornbluh, and Jose P. Joseph. "Electrostriction of polymer dielectrics with compliant electrodes as a means of actuation." *Sensors and Actuators A: Physical* 64, no. 1 (1998): 77-85.
6. Pelrine, Ron, Roy Kornbluh, Jose Joseph, Richard Heydt, Qibing Pei, and Seiki Chiba. "High-field deformation of elastomeric dielectrics for actuators." *Materials Science and Engineering: C* 11, no. 2 (2000): 89-100.
7. Biddiss, Elaine, and Tom Chau. "Dielectric elastomers as actuators for upper limb prosthetics: Challenges and opportunities." *Medical engineering & physics* 30, no. 4 (2008): 403-418.

8. Pei, Qibing, Ron Pelrine, Scott Stanford, Roy Kornbluh, and Marcus Rosenthal. "Electroelastomer rolls and their application for biomimetic walking robots." *Synthetic Metals* 135 (2003): 129-131.
9. Kovacs, G., L. Düring, S. Michel, and G. Terrasi. "Stacked dielectric elastomer actuator for tensile force transmission." *Sensors and Actuators A: Physical* 155, no. 2 (2009): 299-307.
10. Carpi, Federico, and Danilo De Rossi. "Dielectric elastomer cylindrical actuators: electromechanical modelling and experimental evaluation." *Materials Science and Engineering: C* 24, no. 4 (2004): 555-562.
11. O'Halloran, Ailish, Fergal O'malley, and Peter McHugh. "A review on dielectric elastomer actuators, technology, applications, and challenges." *Journal of Applied Physics* 104, no. 7 (2008): 071101.
12. Anderson, Iain A., Todd A. Gisby, Thomas G. McKay, Benjamin M. O'Brien, and Emilio P. Calius. "Multi-functional dielectric elastomer artificial muscles for soft and smart machines." *Journal of Applied Physics* 112, no. 4 (2012): 041101.
13. Pelrine, Ron, Roy Kornbluh, Qibing Pei, and Jose Joseph. "High-speed electrically actuated elastomers with strain greater than 100%." *Science* 287, no. 5454 (2000): 836-839.
14. O'Brien, Benjamin M., Emilio P. Calius, Tokushu Inamura, Sheng Q. Xie, and Iain A. Anderson. "Dielectric elastomer switches for smart artificial muscles." *Applied Physics A* 100, no. 2 (2010): 385-389.
15. Carpi, Federico, Claudio Salaris, and Danilo De Rossi. "Folded dielectric elastomer actuators." *Smart Materials and Structures* 16, no. 2 (2007): S300.

16. Kovacs, Gabor, Patrick Lochmatter, and Michael Wissler. "An arm wrestling robot driven by dielectric elastomer actuators." *Smart Materials and Structures* 16, no. 2 (2007): S306.
17. Prahlad, Harsha, Ron Pelrine, Roy Kornbluh, Philip von Guggenberg, Surjit Chhokar, Joseph Eckerle, Marcus Rosenthal, and Neville Bonwit. "Programmable surface deformation: thickness-mode electroactive polymer actuators and their applications." In *Smart Structures and Materials*, pp. 102-113. International Society for Optics and Photonics, 2005.
18. Lee, Jae Ah, Youn Tae Kim, Geoffrey M. Spinks, Dongseok Suh, Xavier Lepró, Mácio D. Lima, Ray H. Baughman, and Seon Jeong Kim. "All-solid-state carbon nanotube torsional and tensile artificial muscles." *Nano letters* 14, no. 5 (2014): 2664-2669.
19. Lima, Márcio D., Na Li, Monica Jung De Andrade, Shaoli Fang, Jiyoung Oh, Geoffrey M. Spinks, Mikhail E. Kozlov et al. "Electrically, chemically, and photonically powered torsional and tensile actuation of hybrid carbon nanotube yarn muscles." *Science* 338, no. 6109 (2012): 928-932.
20. Zheng, Wen, Joselito M. Razal, Philip G. Whitten, Raquel Ovalle-Robles, Gordon G. Wallace, Ray H. Baughman, and Geoffrey M. Spinks. "Artificial muscles based on polypyrrole/carbon nanotube laminates." *Advanced materials* 23, no. 26 (2011): 2966-2970.
21. Spinks, Geoffrey M., Vahid Mottaghitalab, Mehrdad Bahrami-Samani, Philip G. Whitten, and Gordon G. Wallace. "Carbon-Nanotube-Reinforced Polyaniline Fibers for High-Strength Artificial Muscles." *Advanced Materials* 18, no. 5 (2006): 637-640.

22. Lu, Xiaoyan, Adriana Schirokauer, and Jerry Scheinbeim. "Giant electrostrictive response in poly (vinylidene fluoride-hexafluoropropylene) copolymers." *Ultrasonics, Ferroelectrics, and FrEquency Control, IEEE Transactions on* 47, no. 6 (2000): 1291-1295.
23. Casalini, R., and C. M. Roland. "Highly electrostrictive poly (vinylidene fluoride–trifluoroethylene) networks." *Applied Physics Letters* 79, no. 16 (2001): 2627-2629.
24. Parizi, Saman Salemizadeh, Gavin Conley, Tommaso Costanzo, Bob Howell, Axel Mellinger, and Gabriel Caruntu. "Fabrication of BaTiO3/acrylonitrile-butadiene styrene/poly (methyl methacrylate) nanocomposite films for hybrid ferroelectric capacitors." *RSC Advances* 5, no. 93 (2015): 76356-76362.
25. Rao, Yang, S. Ogitani, Paul Kohl, and C. P. Wong. "Novel polymer–ceramic nanocomposite based on high dielectric constant epoxy formula for embedded capacitor application." *Journal of Applied Polymer Science* 83, no. 5 (2002): 1084-1090.
26. Siddabattuni, Sasidhar, and Thomas P. Schuman. "Polymer-ceramic Nanocomposite Dielectrics for Advanced Energy Storage." (2014): 165.
27. Guo, Neng, Sara A. DiBenedetto, Pratyush Tewari, Michael T. Lanagan, Mark A. Ratner, and Tobin J. Marks. "Nanoparticle, size, shape, and interfacial effects on leakage current density, permittivity, and breakdown strength of metal oxide− polyolefin nanocomposites: experiment and theory." *Chemistry of Materials* 22, no. 4 (2010): 1567-1578.
28. Subbiah, Thandavamoorthy, G. S. Bhat, R. W. Tock, S. Parameswaran, and S. S. Ramkumar. "Electrospinning of nanofibers." *Journal of Applied Polymer Science* 96, no. 2 (2005): 557-569.

29. Dai, Yunqian, Wenying Liu, Eric Formo, Yueming Sun, and Younan Xia. "Ceramic nanofibers fabricated by electrospinning and their applications in catalysis, environmental science, and energy technology." *Polymers for Advanced Technologies* 22, no. 3 (2011): 326-338.

30. Fujihara, Kazutoshi, Wee-Eong Teo, Teik-Cheng Lim, and Zuwei Ma. *An introduction to electrospinning and nanofibers*. Vol. 90. Singapore: World Scientific, 2005.

31. Tucker, Nick, Jonathan J. Stanger, Mark P. Staiger, Hussam Razzaq, and Kathleen Hofman. "The History of the Science and Technology of Electrospinning from 1600 to 1995." *Journal of Engineered Fabrics & Fibers (JEFF)* 7, no. 3 (2012).

32. Zeleny, John. "The electrical discharge from liquid points, and a hydrostatic method of measuring the electric intensity at their surfaces." *Physical Review* 3, no. 2 (1914): 69.

33. Arivalagan, K., S. Ravichandran, K. Rangasamy, and E. Karthikeyan. "Nanomaterials and its potential applications." *International Journal of ChemTech Research* 3, no. 2 (2011): 534-538.

34. Spurny, Kvetoslav Rudolfowich, and Jan CM Marijnissen. *Nicolai Albertowich Fuchs: the pioneer of aerosol science: biography*. Delft University Press, 1998.

35. Taylor, Geoffrey. "Disintegration of water drops in an electric field." In *Proceedings of the Royal Society of London A: Mathematical, Physical and Engineering Sciences*, vol. 280, no. 1382, pp. 383-397. The Royal Society, 1964.

36. Nitanan, Todsapon, Praneet Opanasopit, Prasert Akkaramongkolporn, Theerasak Rojanarata, Tanasait Ngawhirunpat, and Pitt Supaphol. "Effects of processing parameters on morphology of electrospun polystyrene nanofibers." *Korean Journal of Chemical Engineering* 29, no. 2 (2012): 173-181.

37. Hasan, Anwarul, Adnan Memic, Nasim Annabi, Monowar Hossain, Arghya Paul, Mehmet R. Dokmeci, Fariba Dehghani, and Ali Khademhosseini. "Electrospun scaffolds for tissue engineering of vascular grafts." *Acta biomaterialia* 10, no. 1 (2014): 11-25.
38. Kenawy, El-Refaie, Gary L. Bowlin, Kevin Mansfield, John Layman, David G. Simpson, Elliot H. Sanders, and Gary E. Wnek. "Release of tetracycline hydrochloride from electrospun poly (ethylene-co-vinylacetate), poly (lactic acid), and a blend." *Journal of controlled release* 81, no. 1 (2002): 57-64.
39. Lei, Tingping, Lei Xu, Zhan Zhan, Jiang Du, Yiwen Jiang, Gaofeng Zheng, Lingyun Wang, and Daoheng Sun. "Direct fabrication of polymer nanofiber membrane for piezoelectric vibration sensor." In *Sensors, 2011 IEEE*, pp. 1367-1370. IEEE, 2011.
40. Persano, Luana, Canan Dagdeviren, Yewang Su, Yihui Zhang, Salvatore Girardo, Dario Pisignano, Yonggang Huang, and John A. Rogers. "High performance piezoelectric devices based on aligned arrays of nanofibers of poly (vinylidenefluoride-co-trifluoroethylene)." *Nature communications* 4 (2013): 1633.
41. Luzio, Alessandro, Eleonora Valeria Canesi, Chiara Bertarelli, and Mario Caironi. "Electrospun polymer fibers for electronic applications." *Materials* 7, no. 2 (2014): 906-947.
42. Dissanayake, M. A. K. L., H. K. D. W. M. N. R. Divarathne, C. A. Thotawatthage, C. B. Dissanayake, G. K. R. Senadeera, and B. M. R. Bandara. "Dye-sensitized solar cells based on electrospun polyacrylonitrile (PAN) nanofibre membrane gel electrolyte." *Electrochimica Acta* 130 (2014): 76-81.

43. Kim, Ji-Un, Sung-Hae Park, Hyong-Ju Choi, Won-Ki Lee, Jin-Kook Lee, and Mi-Ra Kim. "Effect of electrolyte in electrospun poly (vinylidene fluoride-co-hexafluoropropylene) nanofibers on dye-sensitized solar cells." *Solar Energy Materials and Solar Cells* 93, no. 6 (2009): 803-807.
44. Wang, Xianfu, Kai Jiang, and Guozhen Shen. "Flexible fiber energy storage and integrated devices: recent progress and perspectives." *Materials Today* 18, no. 5 (2015): 265-272.
45. Chang, Jiyoung, Michael Dommer, Chieh Chang, and Liwei Lin. "Piezoelectric nanofibers for energy scavenging applications." *Nano Energy* 1, no. 3 (2012): 356-371.
46. Pu, Juan, Xiaojun Yan, Yadong Jiang, Chieh Chang, and Liwei Lin. "Piezoelectric actuation of direct-write electrospun fibers." *Sensors and Actuators A: Physical* 164, no. 1 (2010): 131-136.
47. Liu, Jie, Xiaolong Lu, and Chunrui Wu. "Effect of Preparation Methods on Crystallization Behavior and Tensile Strength of Poly (vinylidene fluoride) Membranes." *Membranes* 3, no. 4 (2013): 389-405.
48. Huang, Cheng, and Qiming Zhang. "Enhanced Dielectric and Electromechanical Responses in High Dielectric Constant All-Polymer Percolative Composites." *Advanced Functional Materials* 14, no. 5 (2004): 501-506.
49. Jang, Won Gi, Jian Hou, and Hong sik Byun. "Preparation and characterization of PVdF nanofiber ion exchange membrane for the PEMFC application." *Desalination and Water Treatment* 34, no. 1-3 (2011): 315-320.

50. Guo, Yunlong, Gui Yu, and Yunqi Liu. "Functional Organic Field-Effect Transistors." *Advanced Materials* 22, no. 40 (2010): 4427-4447.
51. Gerber, A., M. Fitsilis, R. Waser, Timothy J. Reece, E. Rije, Stephen Ducharme, and H. Kohlstedt. "Ferroelectric field effect transistors using very thin ferroelectric polyvinylidene fluoride copolymer films as gate dielectrics." *Journal of applied physics* 107, no. 12 (2010): 124119.
52. Parizi, Saman Salemizadeh, Axel Mellinger, and Gabriel Caruntu. "Ferroelectric BaTiO3 Nanocubes as Capacitive Building Blocks for Energy Storage Applications." *ACS applied materials & interfaces* 6, no. 20 (2014): 17506-17517.
53. Desai, Tapan, Pawel Keblinski, and Sanat K. Kumar. "Molecular dynamics simulations of polymer transport in nanocomposites." *The Journal of chemical physics* 122, no. 13 (2005): 134910.
54. Atkinson, K. E., and C. Jones. "A study of the interphase region in carbon fibre/epoxy composites using dynamic mechanical thermal analysis." *The Journal of Adhesion* 56, no. 1-4 (1996): 247-260.
55. Baniasadi, Mahmoud, Jiacheng Huang, Zhe Xu, Salvador Moreno, Xi Yang, Jason Chang, Manuel Angel Quevedo-Lopez, Mohammad Naraghi, and Majid Minary-Jolandan. "High-Performance Coils and Yarns of Polymeric Piezoelectric Nanofibers." *ACS applied materials & interfaces* 7, no. 9 (2015): 5358-5366.